Equation of state for solids considering cohesive energy and anharmonic effect and its application to MgO*

Zhang Da(张 达)[a] and Sun Jiu-Xun(孙久勋)[a)b)†]

[a] *Department of Applied Physics, University of Electronic Science and Technology of China, Chengdu* 610054, *China*

[b] *Laboratory for Shock Wave and Detonation Physics Research, Southwest Institute of Fluid Physics, Mianyang* 621900, *China*

(Received 5 December 2011; revised manuscript received 6 January 2012)

A simple equation of state (EOS) in wide ranges of pressure and temperature is constructed within the Mie–Grüneisen–Debye framework. Instead of the popular Birch–Murnaghan and Vinet EOS, we employ a five-parameter cold energy expression to represent the static EOS term, which can correctly produce cohesive energy without any spurious oscillations in the extreme compression and expansion regions. We developed a Padé approximation-based analytic Debye quasiharmonic model with high accuracy which improves the performance of EOS in the low temperature region. The anharmonic effect is taken into account by using a semi-empirical approach. Its reasonability is verified by the fact that the total thermal pressure tends to the lowest-order anharmonic expansion in the literature at low temperature, and tends to ideal-gas limitation at high temperature, which is physically correct. Besides, based on this approach, the anharmonic thermal pressure can be expressed in the Grüneisen form, which is convenient for applications. The proposed EOS is used to study the thermodynamic properties of MgO including static and shock compression conditions, and the results are very satisfactory as compared with the experimental data.

Keywords: equation of state, cohesive energy, anharmonic effect, high temperature and pressure

PACS: 05.70.Ce, 64.30.Jk, 62.50.–p **DOI:** 10.1088/1674-1056/21/8/080508

1. Introduction

Characterized by describing the relationships among the thermodynamic variables of compressed solids, equation of state (EOS) becomes a crucial concept in the investigations of material properties and high-pressure physics studies, in which the isothermal $P(V,T)$ relation is of most importance. Over the past decades, many EOSs have been proposed with varying extents of success.[1−10] Whereas, the recent studies of Li *et al.*,[7,8] Qin *et al.*,[9,10] and our calculations[11−13] exhibit that firstly, the EOSs proposed by Murnaghan, Boanza *et al.*,[4,5] and Holzapfel[6] cannot give physically reasonable cohesive energy; secondly, the cohesive energy values deduced from the Vinet[3] (the extended Rydberg EOS as pointed out by Qin *et al.*[9,10]), third-order Birch–Murnaghan and Rose[1,2] EOSs deviate from experimental observation. Besides, Qin *et al.*[9,10] pointed out that the physically incorrect oscillations existed in the fourth-order Birch–Murnaghan EOS for some materials in extreme compression regions. We[14] also noticed that the same problem existed in Li *et al.*'s[7,8] EOS. Both incorrect oscillations result from the higher-order terms in their EOSs. The unphysical oscillations would bring on unreliable results in the studies of the thermodynamics in extreme conditions. In order to solve the problem, we proposed a generalized exponential function (GEF) type EOS in Ref. [14], which can incorporate cohesive energy data, and there are no longer physically incorrect oscillations existing in all pressure regions.

MgO is one of the major earth-forming minerals. It plays a key role in understanding the thermophysical properties of the earth's lower mantle. Also with the NaCl-type structure stability, MgO becomes an ideal pressure scale applied in DAC experiments under extreme conditions.[15] Important in high temperature and pressure research, the $P(V,T)$ EOS of MgO has been widely studied theoretically[16−26] and experimentally.[27−34] In recent theoretical stud-

*Project supported by the Joint Fund of National Natural Science Foundation of China and China Academy of Engineering Physics (Grant No. 10876008).

†Corresponding author. E-mail: sjx@uestc.edu.cn

© 2012 Chinese Physical Society and IOP Publishing Ltd

ies for MgO, the Birch–Murnaghan and Vinet EOS are most popular to represent cold energy, which probably involve some shortcomings mentioned above. In most of the present theoretical research, the Einstein model, rather than the more precise Debye model, is used to calculate the harmonic thermal contribution. Moreover, the anharmonic effect is taken into account by using the lowest-order high-temperature expansion.[19,22,23,26,35–37] However, Shukla *et al.*[38,39] have shown that the anharmonic expansion is divergent at high temperature, thus it is necessary to adopt a more appropriate approach to consider the anharmonic effect.

In this work, we construct a simple $P(V,T)$ EOS for MgO within the Mie–Grüneisen–Debye framework, in which three main issues are addressed: firstly, the proposed GEF EOS in Ref. [14] is employed to build the cold energy of our thermal EOS to overcome the shortcomings mentioned above; secondly, an analytic approximation to the Debye model is developed with high accuracy to describe the quasiharmonic term of thermal energy; thirdly, a model for the anharmonic effect is proposed with the merit that it approaches anharmonic expansion at low temperature, and tends to the ideal gas model at high temperature. Then we use the proposed $P(V,T)$ model to study the thermodynamic characteristics of MgO in wide temperature and pressure ranges, including static compression, shock compression, thermal expansion, thermal expansion coefficient, volume modulus, and heat capacity together with their comparisons with experimental data. The results are very satisfactory and confirm the validity of the proposed $P(V,T)$ EOS.

2. Construction of EOS

The total Helmholtz free energy of solids can be expressed as the sum of the following terms:

$$F = E_{\rm c}(V) + F_{\rm h}(T,V) + F_{\rm a}(T,V), \tag{1}$$

where $E_{\rm c}(V)$ is the cohesive energy at 0 K; $F_{\rm h}(T,V)$ and $F_{\rm a}(T,V)$ are the quasiharmonic and anharmonic parts of the Helmholtz free energy, respectively.[22] Considering the large energy band gap of MgO, we neglect the thermal electronic excitation in Eq. (1), so the total pressure is evaluated by differentiating Eq. (1) as follows:

$$P = -\Big(\frac{\partial F}{\partial V}\Big)_T = P_{\rm c}(V) + P_{\rm h}(T,V) + P_{\rm a}(T,V), \tag{2}$$

where $P_{\rm c}(V)$ is the cold pressure; $P_{\rm h}(T,V)$ and $P_{\rm a}(T,V)$ are the quasiharmonic and anharmonic parts of the pressure respectively.

2.1. Cold EOS

The Birch–Murnaghan[19,23,25,26,31] EOS and Vinet[15,22] EOS are most popular to describe the cold energy of MgO. However, to overcome the unphysical oscillations in the former and the incorrect cohesive energy induced from the latter, Qin *et al.*,[9,10] Sun *et al.*,[11] and we[14] proposed two EOSs to solve these problems respectively. The equations of cold energy and EOS proposed by Qin *et al.*[9,10] are as follows:

$$E_{\rm c} = Ax^{-m}\,{\rm e}^{\alpha(1-X)} - Bx^{n}\,{\rm e}^{\beta(1-X)}, \tag{3}$$

$$P_{\rm c} = \frac{3B_0}{CX^2}\big[(\alpha+m/X)(\beta-n)X^{-m}\,{\rm e}^{\alpha(1-X)} - (\alpha+m)(\beta-n/X)X^{n}\,{\rm e}^{\beta(1-X)}\big]. \tag{4}$$

Here, A, B, and C can be expressed as

$$A = 9B_0V_0(\beta-n)/C, \tag{5}$$

$$B = 9B_0V_0(\alpha+m)/C, \tag{6}$$

$$C = (\alpha+m)(\beta-n)[(\alpha+m)-(\beta-n)] + (\alpha n+\beta m). \tag{7}$$

The EOS of Qin *et al.*[9,10] contains six parameters V_0, B_0, α, β, m, and n. V_0 and B_0 are the molar volume and the bulk modulus at zero pressure; $X = (V/V)^{1/3}$ is the normalized volume. Qin *et al.*[9,10] applied their EOS to nine 4d and nine 5d transition metals, separately, to study variation of parameters with atomic number. Their results show that equation (3) can describe binding-energy data well from density-functional theory (DFT) calculations, and there is no unphysical oscillation at high pressure.

However, as we used Eq. (6) of Qin *et al.* to fit experimental compression data at high pressure taking the experimental cohesive energy into account, we found some inconsistence in that optimizing the fitting error of the pressure always enlarges the fitting error of the cohesive energy, and *vise versa*. Otherwise, we notice that among 18 transition metals studied by Qin *et al.*,[9,10] the values of parameter α of 7 metals are all taken to be zero values while the values of their parameter β are adopted to be large values, which may result in abnormal maximum in the expansion regions for the 7 metals; yet this case does not happen in the remaining 11 metals.

Therefore, we propose other EOSs as an alterna-

tive to Eqs. (3) and (4) of Qin *et al.*[10,11]

$$E_{\rm c} = (E_0\alpha)\left[n\beta\,{\rm e}^{\alpha(1-X)} - n\beta - \alpha\right]{\rm e}^{\beta(1-X^n)}, \quad (8)$$

$$P_{\rm c} = \frac{n\beta E_0}{3\alpha V_0 X^3}\left[(\alpha X + n\beta X^n)\,{\rm e}^{\alpha(1-X)} - (\alpha + n\beta)X^n\right]{\rm e}^{\beta(1-X^n)}, \quad (9)$$

which for convenience is called generalized exponential function (GEF) EOS. It contains five parameters, V_0, E_0, α, β, and n, with the number of parameters less than that of Eq. (6) of Qin *et al.* Here E_0 is the binding energy at zero pressure. It is apparent that the repulsive part $n\beta\exp[\alpha(1-X)+\beta(1-X^n)]$ in Eq. (8) is a monotonically decreasing function of X; the attractive part $(-n\beta-\alpha)\exp[\beta(1-X^n)]$ is the monotonically increasing function of X. Being the sum of these two parts, the potential function Eq. (8) therefore has one unique minimum at $X = 1$, and the corresponding GEF EOS in Eq. (9) is physically correct without any unreasonable oscillation in either high pressure or expanding regions. Moreover, the inclusion of E_0 in Eq. (8) guarantees that the GEF EOS can yield correct binding energy, if its value is adopted from experimental data.

2.2. Debye quasiharmonic vibrational energy

Based on the Mie–Grüneisen approach, the quasiharmonic thermal pressure $P_{\rm h}(T,V)$ can be expressed as the Grüneisen form both in Einstein and Debye models

$$P_{\rm h}(T,V) = \gamma_{\rm G}\frac{U_{\rm h}(T,V)}{V}, \quad (10)$$

where $\gamma_{\rm G}$ is the Grüneisen coefficient, and $U_{\rm h}(T,V)$ is the quasiharmonic internal energy. Because the $U_{\rm h}(T,V)$ can be expressed as a simple function in the Einstein model but cannot in the Debye model, the Einstein model is used widely in the literature,[19,21,23,25,26,31] although the Debye model is more accurate. To balance accuracy and computational efficiency, several authors[22,36,37] have developed pseudo-Debye models to express $U_{\rm h}(T,V)$ as an approximate analytic function.

However, those pseudo-Debye models[22,36,37] are not accurate enough for most applications, so we develop a new pseudo-Debye model with high accuracy in light of the Padé approximation. The quasiharmonic internal energy in the Debye model can be expressed as

$$U_{\rm h} = 3nRT\left[\frac{3}{8}x + 3x^{-3}\int_0^x ({\rm e}^y - 1)^{-1}y^3\,{\rm d}y\right]. \quad (11)$$

Here R is the ideal gas constant per mole, n is the number of atoms per cell ($n = 2$ for MgO), $y = h\omega/kT$, and $x = \Theta_{\rm D}/T$. We use the following Padé approximation to fit Eq. (11):

$$3x^{-3}\int_0^x ({\rm e}^y - 1)^{-1}y^3\,{\rm d}y \approx (1 + b_0 x)\varphi^{-1}(x). \quad (12)$$

Here, $\varphi(x) = 1 + b_1 x + b_2 x^2 + b_3 x^3 + b_4 x^4$. We can easily obtain the optimized coefficients b_i ($i = 0\sim4$), and thus we have

$$U_{\rm h} = 3nRT[3x/8 + (1 + x/4)\varphi^{-1}(x)], \quad (13)$$

$$\varphi(x) = 1 + x/4 + 5x^2/8 + 3x^3/16 + 5x^4/4\pi^4, \quad (14)$$

$$C_{\rm Vh} = 3nR[\varphi(x) + x(1 + x/4)\varphi'(x)]\varphi^{-2}(x). \quad (15)$$

In Fig. 1, we compare the heat capacity calculated by using the approximate formula in Eq. (15) with the exact results of the Debye integral. Figure 1 shows that the results from the approximate formula are in good agreement with the exact results which confirms the validity of the proposed approximation.

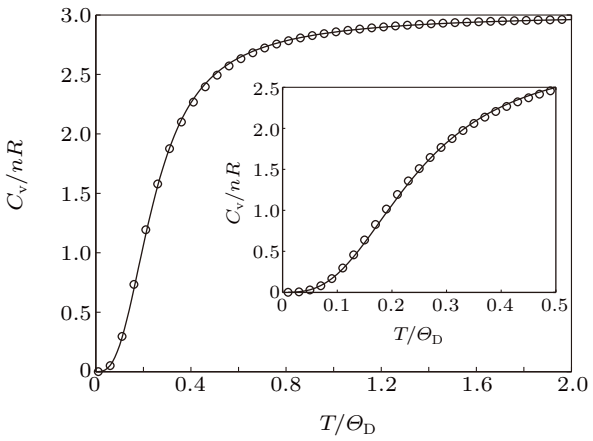


Fig. 1. Heat capacity at constant volume. The circles denote the results from the exact Debye model; the solid line represents the data from our analytic approximation. The inset shows the comparison in the low temperature region.

As for the Grüneisen parameter $\gamma_{\rm G}$, we employ the form suggested by Al'tshuler *et al.*[40] and Vorobev,[41] which is expressed as

$$\gamma_{\rm G} = \gamma_\infty + (\gamma_0 - \gamma_\infty)(V/V_0)^\lambda, \quad (16)$$

where γ_0 and γ_∞ are the values of the Grüneisen parameter at ambient conditions and infinite compression respectively, and λ is a fitted parameter. Integrating the relation $\gamma_{\rm G} = {\rm d}\ln\Theta_{\rm D}/{\rm d}\ln V$, we have the Debye temperature

$$\Theta_{\rm D} = \Theta_{\rm D0}(V_0/V)^{\gamma_\infty}\exp\{\lambda^{-1}(\gamma_0 - \gamma_\infty) \times [1 - (V/V_0)^\lambda]\}, \quad (17)$$

in which $\Theta_{\rm D0}$ is the Debye temperature in ambient condition.

2.3. Anharmonic model

It is well known that the anharmonic effect becomes very important at high temperature (especially at low compression conditions).[22,36,37] The lowest-order term in the high temperature expansion of anharmonic free energy is quadratic[19,22,23,26,35–37] as follows:

$$F_{\rm a} = \frac{3}{2} nRa_0 (V/V_0)^m T^2. \tag{18}$$

The equation contains two parameters a_0 and m. Correspondingly, the anharmonic heat capacity is

$$C_{\rm Va} = 3nRa_0 (V/V_0)^m T. \tag{19}$$

Recently, Dorogokupets and Oganov[22,36] proposed the quantum anharmonic expansion which approaches Eq. (16) at high temperature. However, Lacks and Shukla,[39] and Al'tshuler *et al.*[40] have shown that the anharmonic expansion is divergent at high temperature, which suggests that equations (18) and (19) are incorrect at high temperature. In addition, we notice that the anharmonic thermal pressure $P_{\rm h}(T, V)$ cannot be expressed as the Grüneisen form whether based on the anharmonic expansion or in light of the free volume theory (FVT). This is not convenient for practical applications.

Hence, we propose a simple semi-empirical approximation to consider the anharmonic effect. Grover[42] pointed out that $C_{\rm V}$ of liquid metal above melting point can be on the average approximated simply by the same linearly decreasing function of temperature. Xu and Zhang[43] further modified the dependence of $C_{\rm V}$ on temperature as

$$C_{\rm V} = \frac{3}{2} nR\big[1 + (1 + \delta T/T_{\rm m})^{-1}\big], \tag{20}$$

where $T_{\rm m}$ is the melting temperature at a constant pressure; δ is an adjusted parameter evaluated at 0.1 to achieve the best agreement with the simulation results. Although equation (20) is proposed incipiently for liquid metals, we think, it can be also applied to solids approximately, because of the similarity of the neighbourhood arrangements of atoms in solids and in liquids. For example, although the FVT is proposed incipiently for liquids, it is mainly applied to solids at present. Moreover, at high temperature and pressure, all matters become fluid states, and the difference between solids and liquids tends to disappear.

For simplicity, we modify Eq. (20) to a slightly different form as follows:

$$C_{\rm V} = \frac{3}{2} nR\big[1 + (1 + \delta T/T_{\rm m})^{-2}\big], \tag{21}$$

where δ is modified as 0.06 to fit Eq. (20) correspondingly. In order to separate the anharmonic part, equation (21) is decomposed as follows:

$$C_{\rm V} = 3nR + \frac{3}{2} nR[-1 + (1 + \delta T/T_{\rm m})^{-2}]. \tag{22}$$

It is apparent that the first term on the right-hand side of the above expression is the Dulong–Petit law; the second term is the anharmonic heat capacity

$$C_{\rm Va} = \frac{3}{2} nR[-1 + (1 + \delta T/T_{\rm m})^{-2}]. \tag{23}$$

Now we explain the reasonability of Eq. (23). First, incorporating Eq. (21) it is evident that the heat capacity tends to be a finite value of ideal gas limitation at high temperature limitation, which is reasonable; nevertheless, the heat capacity based on the anharmonic expansion in Eq. (19) diverges at extremely high temperature, which is physically incorrect. Second, equation (23) would reduce into $C_{\rm Va} = -3nR(\delta T/T_{\rm m})$ at low temperature, and this is in agreement with the anharmonic expansion in Eq. (19). Third, equation (23) is seemingly dependent on melting temperature $T_{\rm m}$, but $T_{\rm m}$ is a function of volume V; therefore, $T_{\rm m}$ mainly control the variation of $C_{\rm Va}$ with V. In addition, the reasonability can be also verified by the fact that the total thermal pressure would tend to ideal gas limitation in both high temperature and low density ($V \to \infty$) condition, which will be stated in the following paragraph. However, the anharmonic expansion models do not have such merits, and are unreasonable.

In terms of thermodynamic relationships and Eq. (23), the anharmonic contributions to the internal energy, free energy, and thermal pressure can be derived as follows:

$$\begin{aligned} U_{\rm a} &= \int_0^T C_{\rm V}\,{\rm d}T = \frac{3}{2} nR \int_0^T \big[-1 + (1 + \delta T/T_{\rm m})^{-2}\big]\,{\rm d}T \\ &= -\frac{3}{2} nRT(1 + T_{\rm m}/\delta T)^{-1}, \end{aligned} \tag{24}$$

$$\begin{aligned} F_{\rm a} &= -T \int \frac{U_{\rm a}}{T^2}\,{\rm d}T \\ &= -\frac{3}{2} nRT \int (\delta T/T_{\rm m})[1 + T_{\rm m}/(\delta T)]^{-1}\,{\rm d}[T_{\rm m}/(\delta T)] \\ &= \frac{3}{2} nRT \ln(1 + \delta T/T_{\rm m}), \end{aligned} \tag{25}$$

$$P_{\rm a} = -\frac{\partial F_{\rm a}}{\partial V} = -\frac{U_{\rm a}}{T_{\rm m}} \frac{\partial T_{\rm m}}{\partial V}$$

$$= -\frac{V}{T_{\rm m}}\frac{\partial T_{\rm m}}{\partial V}\frac{U_{\rm a}}{V} = \gamma_{\rm a}\frac{U_{\rm a}}{V} \quad (26)$$

In Eq. (26), $\gamma_{\rm a} = {\rm d}\ln T_{\rm m}/{\rm d}\ln V$. According to the Lindermann melting law $T_{\rm m} = cM\Theta_{\rm D}^2 V^{2/3}$, we obtain

$$\gamma_{\rm a} = 2\gamma_{\rm G} - 2/3. \quad (27)$$

Comparing Eq. (26) with Eq. (10), we know that the anharmonic thermal pressure has the same form as the quasiharmonic part; both can be expressed as a simple Grüneisen form, and this is very convenient for practical applications. Otherwise, in terms of Eqs. (10), (24), (26), and (27), it can be seen that at high temperature $U_{\rm a} \to -3/2nRT$. In terms of the Lindermann melting law and Eqs. (10), (13), (14), (24), (26), and (27), it can be seen that at low density ($V \to \infty$), $\Theta_{\rm D} \to 0$, $T_{\rm m} \to 0$ and also $U_{\rm a} \to -3/2nRT$. Thus, the total thermal pressure ($P_{\rm h} + P_{\rm a}$) tends to ideal gas EOS nRT/V in both cases.

3. Results and discussion

Substituting Eqs. (4), (10), and (26) into Eq. (2), we obtain the analytic $P(V,T)$ EOS. Now we use this EOS to discuss some important thermodynamic behaviours of MgO. There are a total of ten input parameters E_0, V_0, γ_0, γ_∞, λ, $\Theta_{\rm D0}$, $T_{\rm m0}$, α, β, and n in the proposed EOS. Of them the first seven ones should be cited from experimental or empirical data, and their values are given in Table 1 where, for comparison, values from other versions of EOS are listed too. The remaining three α, β, and n, via the least square procedure, are determined by fitting the calculated EOS to the measured data of the compression at room temperature and the expansion at high temperature simultaneously, which are rich in experimental observations; the best fitted values are 10.2118, 0.3466, and 4.3646 respectively.

Table 1. Input parameters for ours, Wu *et al.*'s,[23] and Tange *et al.*'s[25] EOSs. The units are as follows: E_0 in kJ·mol^{-1}, V_0 in cm^3·mol^{-1}, $\Theta_{\rm D0}$ and $T_{\rm m0}$ in K and B_0 in GPa.

Ours[a]	γ_0	γ_∞	λ	$\Theta_{\rm D0}$	V_0	E_0	α	β	n	$T_{\rm m0}$
	1.520	0.606	1.406	747[b]	11.19[c] [0 K] 11.244[d] [298 K]	725[e]	10.212	0.3466	4.3646	3000[f]
Wu *et al.*[20]	γ_0	γ_∞	λ	$\Theta_{\rm E0}$	V_0	B_0	B_0'	a	m	—
	1.520	0.606	1.406	621	11.248	162.2	4.23	−15.4	1.75	—
Tange *et al.*[21]	γ_0	γ_∞	λ	$\Theta_{\rm E0}$	V_0	B_0	B_0'	a	m	—
	1.431	1.016	3.5	589	11.248	160.64	4.221	—	—	—

[a] Apart from the values of E_0 and V_0 in our EOS, other parameters are at 298 K. γ_0, γ_∞, and λ in our EOS are not measured but cited from the fitted values of Wu *et al.*'s.[23]; [b]Ref. [44]; [c]Fitted parameter from Ref. [19]; [d]Ref. [19]; [e]Ref. [45]; [f]Ref. [46].

Of varying types of EOSs, the version of Speziale *et al.*[31] based on the Birch–Murnaghan EOS within the Mie–Grüneisen–Einstein framework is most often used.[26] Below, we choose as the contrasts the versions of Speziale *et al.*'s[31] EOS employed by Wu *et al.*[23] and Tange *et al.*[25] Therein, the former also incorporates anharmonicity. Wu *et al.*'s[23] $P(V,T)$ EOS is expressed as

$$\begin{aligned} P = {} & \frac{3}{2}B_0\left(x^{-7/3} - x^{-5/3}\right) \\ & \times \left[1 - (3/4)(4 - B_0')(x^{-2/3} - 1)\right] \\ & + \frac{3n\lambda R\Theta_0}{V}\left[\left({\rm e}^{\Theta_0/T} - 1\right)^{-1} - \left({\rm e}^{\Theta_0/T_0} - 1\right)^{-1}\right] \\ & + \frac{3nRa_0m}{2V}\left(T^2 - T_0^2\right)x^m. \end{aligned} \quad (28)$$

The first, second, and third lines are the static, quasiharmonic, and anharmonic terms respectively; the definitions of γ and Θ are the same as those in Eqs. (16) and (17). The Tange *et al.*'s version[25] does not have the third term. It should be noted that B_0 and B_0' here are set as their values at the reference temperature T_0; namely, the first line of Eq. (25) represents the isotherm at T_0, which differs from the definitions of Eqs. (8) and (9). In addition, because our calculation method is rooted from empirical thermodynamics, the comparisons with the simulation methods[17−21,24] will not be made here.

Figure 2 shows the calculated 300-K isotherms based on the EOSs of ours together with Wu *et al.*'s[23] and Tange *et al.*'s,[25] and the comparison with the experimental data[27,31,34] up to about 225 GPa. It can be seen that below 150 GPa, all the three calculated results match the experimental data well; upon 150 GPa, Wu *et al.*'s[23] and Tange *et al.*'s[25] results nearly overlap but deviate from our results. However, it seems that only our results are located averagely in the middle of the scattering experimental data by Duffy *et al.*,[27] which implies that our EOS might have more correct behaviour in the higher pressure region. The same comparison of only our results as in

Fig. 2 but for the data at 1473 K, 1673 K, 1873 K, and 2173 K[29,47] is shown in Fig. 3, indicating that our results are in good agreement with the experimental data, thereby confirming the capability of our EOS to predict compression at high temperatures. Besides, the Hugoniot compression and shock wave versus particle velocity relationship of our EOS are compared with observation data[48−50] in Figs. 4 and 5 respectively, and both obtain good fits.

Figure 6 shows the dependences of bulk modulus on temperature at ambient pressure $B_0(T)$ obtained from ours, Wu *et al.*'s,[23] and Tange *et al.*'s[25] EOSs, compared with the experimental data.[51−54] Within the range of the experimental data, the largest relative error (from Wu *et al.*'s[23] model) is no more than 3.5%, which indicates the good fit of all three models. Because the experimental data are of scarcity beyond 1500 K, further studies are expected.

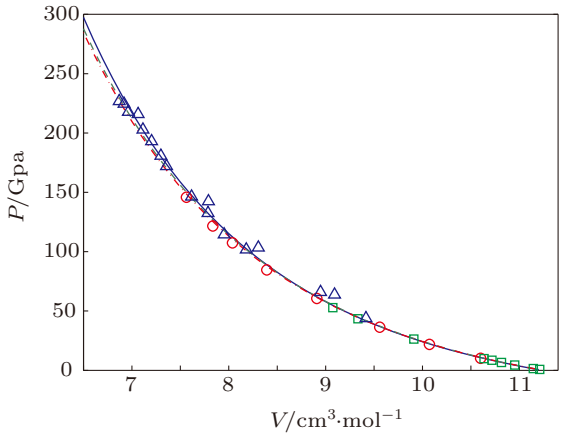


Fig. 2. (colour online) The isotherm of MgO at 300 K. Calculated results: solid line-ours; dashed line-Wu *et al.*'s;[23] dot-dashed line-Tange *et al.*'s.[25] Measured results: squares-Ref. [31]; circles-Ref. [34]; triangles-Ref. [27].

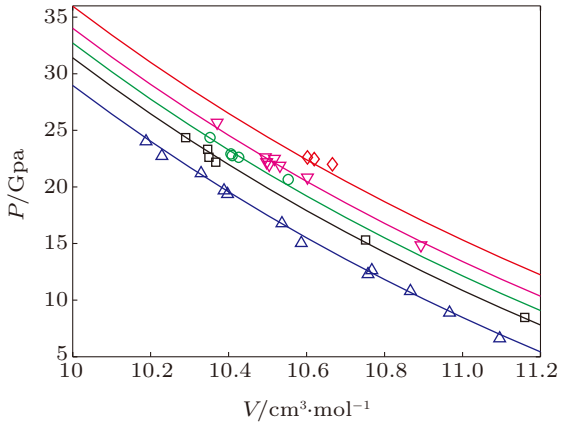


Fig. 3. (colour online) Isotherms of MgO at high temperatures. Solid lines denote the calculated results from our EOS. Experimental data: upward triangles at 1100 K–Ref. [29]; all of squares at 1473 K, circles at 1673 K, downward triangles at 1873 K, and diamonds at 2173 K–Ref. [47].

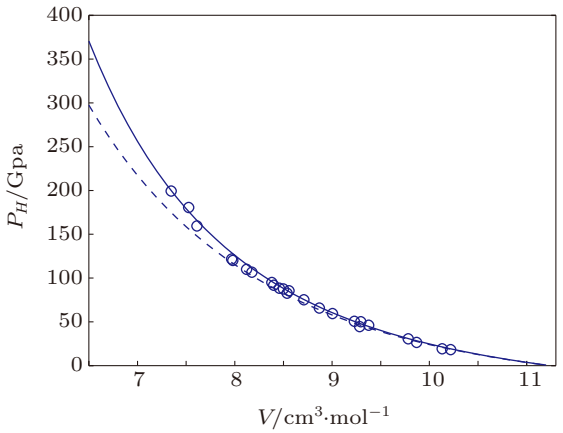


Fig. 4. (colour online) Hugoniot compression of MgO derived from our EOS. The 300-K isotherm is also plotted to illustrate the relative thermal pressure. Experimental data are cited from Refs. [48] and [49].

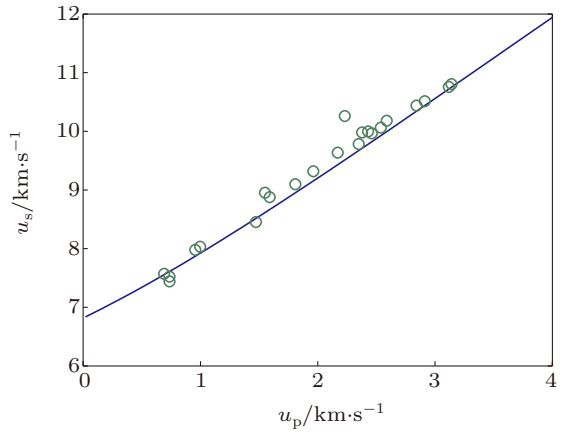


Fig. 5. (colour online) Shock sound wave velocity (u_s) as a function of particle velocity (u_p) for the shock Hugoniot. Experimental records are cited from Refs. [48] and [50].

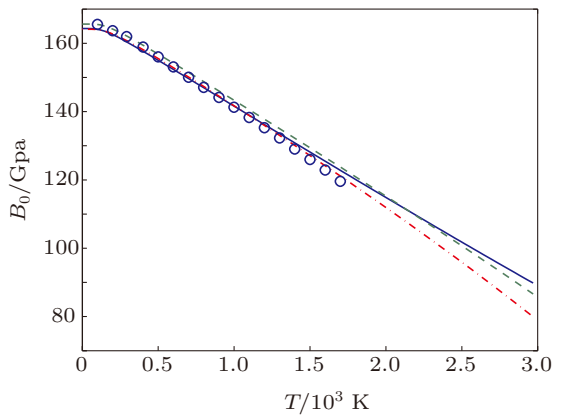


Fig. 6. (colour online) Bulk modulus at ambient pressure as a function of temperature. Calculated results: solid line-ours; dashed line-Wu *et al.*'s;[23] dot-dashed line-Tange *et al.*'s.[25] Measured results are cited from Refs. [51]–[54].

Figure 7 shows the comparison between the experimental data[51−53] and the calculated V–T at ambient

pressure based on ours, Wu *et al.*'s,[23] and Tange *et al.*'s[25] EOSs, and the predicted results at high temperature. Over the whole temperature range of the measured data, all the models have good fits. However, it is obvious from the inset that Wu *et al.*'s[23] and Tange *et al.*'s[25] results deviate slightly from the observations at the low temperatures while our results match them well, for which the reason will be stated below. B_0 and B_0' in Eq. (28) are set as their values at the reference temperature T_0, so that the static term [the first line of Eq. (28)] contains the thermal contribution at T_0. To satisfy the zero-pressure condition $P(V_0, T_0) = 0$, this T_0 contribution needs to be extracted from the thermal terms, i.e., the second terms of the second and third lines of Eq. (28). The problem is that this 'extraction' is not accurate, resulting in the fact that $P(V_0, T_0) = 0$ is actually not satisfied for Eq. (28); hence the calculated equilibrium volume is inaccurate. On the contrary, we set our input parameter V_0 and E_0 as their values at 0 K estimated according to the observation records, thereby effectively solving this problem .

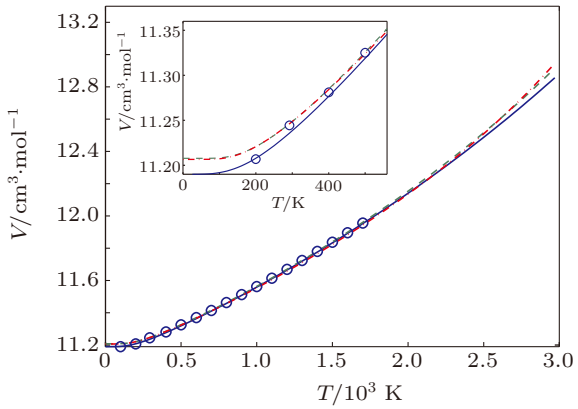


Fig. 7. (colour online) Isotonics at ambient pressure. Calculated results: solid line-ours; dashed line-Wu *et al.*'s;[23] dot-dashed line-Tange *et al.*'s.[25] Measured data are cited from Refs. [51]–[53].

Figure 8 shows the comparisons of the dependence of thermal expansion coefficients on temperature $\alpha(T)$ with the experimental observations.[55,56] It can be seen that over the whole temperature range, the results of our EOS are in the best agreement with the experimental data; especially in the region from 1500 K to 3000 K, the results of Tange *et al.*'s[25] EOS without considering the anharmonicity diverge rapidly; the performance of Wu *et al.*'s[23] results is not good enough despite considering the anharmonicity by the anharmonic expansion method; in contrast, our EOS closely reproduces the experimental data, which, from another angle, proves the good prediction of high temperature expansion of our model, owing to the proposed treatment of intrinsic anharmonicity. Furthermore, although our EOS is fitted within the temperature range only to 1800 K (data in Fig. 7), figure 8 reveals that our EOS is still well-behaved while extrapolated into the higher temperature region.

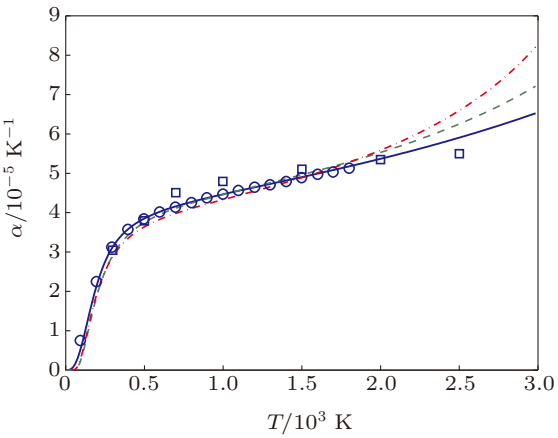


Fig. 8. (colour online) Variations of the thermal expansion coefficient with temperature for MgO. Calculated results: solid line-ours; dashed line-Wu *et al.*'s;[23] dot-dashed line-Tange *et al.*'s.[25] Experimental data: circles–Ref. [55]; squares–Ref. [56]. The data from Ref. [55] are consistent with the thermal expansion measurements in Fig. 7, so below 1800 K, this series of data should be the benchmark here.

It is very meaningful to investigate the specific heat capacity at constant pressure C_P and that at constant volume C_V especially in two extreme conditions: the low temperature region where the quasi-harmonic model dominates and the high temperature region where the anharmonic effect emerges. Figure 9 shows the comparison of $C_\mathrm{P}(T)$ between the experimental data[51–53,57] and calculations by ours, Wu *et al.*'s,[23] and Tange *et al.*'s[25] EOS and that of $C_\mathrm{V}(T)$ between the experimental data[51–53,57] and only our results from EOS. The inset in Fig. 9(b) shows the same but more detailed content of $C_\mathrm{V}(T)$ at low temperature. It is revealed from Fig. 9(a) that $C_\mathrm{P}(T)$ from our EOS matches the experimental data excellently over the whole temperature range; the results from Tange *et al.*'s[25] EOS omitting the intrinsic anharmonicity diverge at high temperature expectedly; yet the results from Dorogokupets and Oganov's [22] EOS deviate from the experimental data despite including the anharmonicity. Figure 9(b) shows that with the temperature increasing, $C_\mathrm{V}(T)$ from our EOS deviates from Dulong–Petit limit yet matches the experimental data, which also confirms the validity and necessity of our anharmonic model. Otherwise, the inset shows that in the low temperature region, the results

from both Wu *et al.*'s[23] and Tange *et al.*'s[25] EOSs decrease too rapidly compared with the experimental data, which originates from the poor performance of the Einstein model at low temperature; however, our pseudo-Debye model has a correct T^3 behaviour and accords well with the experimental data.

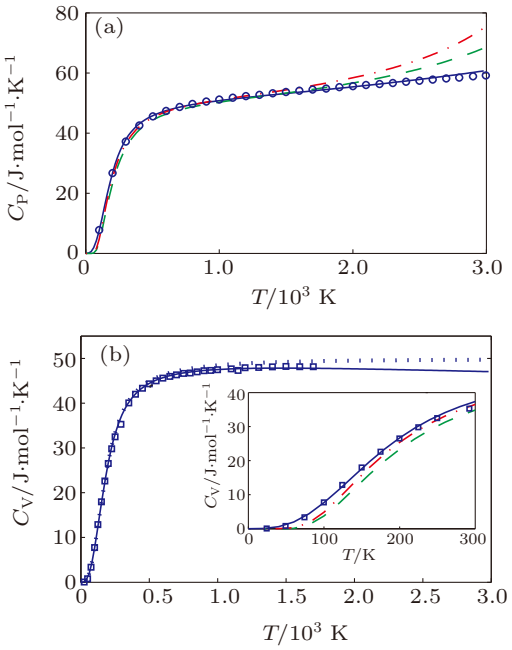


Fig. 9. (colour online) Specific heat capacities at ambient pressure each as a function of temperature. (a) At constant pressure C_P. Calculated results: solid line-ours; dashed line-Dorogokupets and Oganov's;[22] dot–dashed line-Tange *et al.*'s.[25] Experimental data are cited from Ref. [57]. (b) At constant volume C_V from our EOS. Dotted line–without the harmonicity; solid line–with the harmonicity. Experimental data are cited from Refs. [51]–[53].

4. Conclusions

We proposed an analytic $P(V,T)$ EOS within the Mie–Grüneisen–Debye framework. When considering the static EOS, we use a proposed cold energy model published in our previous work[14] which correctly incorporates cohesive energy data without physically incorrect oscillations in both extreme high pressure and expansion regions. Afterwards, a Padé approximation-based analytic Debye quasiharmonic model is addressed with good agreement with the Debye integral. For the intrinsic anharmonicity, unlike the classical expansion treatment involving fitted parameters, we introduce a semi-empirical method with following merits: first, it employs only two measurable variables T_m and γ_{qh}; second, it guarantees the correct behaviour at low and high temperature limitations; finally, the anharmonic contribution to thermal pressure can be expressed in the Grüneisen form, which is convenient for applications. Based on the proposed $P(V,T)$ EOS, we compared the calculated thermodynamic properties of MgO with the experimental results; meanwhile, as contrast, two counterparts from Wu *et al.*'s[23] and Tange *et al.*'s[25] models are compared together.

For the aspect of compression characteristics, all the comparisons of 300-K isotherm, isotherms at different high temperatures, temperature dependence of bulk modulus and Hugoniot show good agreement between our model and measured data. Especially the comparison of 300-K isotherm beyond 150 GPa suggests that our model has more correct behaviour in the future high pressure region than the contrast models.

For the aspect of expansion characteristics, we compare with the measured data the V–T relation at ambient pressure, the thermal expansion coefficient $\alpha(T)$ and the specific heat capacity $C_V(T)$ and $C_P(T)$. There are three points to be addressed. Firstly, if the static EOS is not set as the corresponding 0 K isotherm but as the isotherm at reference temperature T_0, the calculated equilibrium volume at low temperatures will be inaccurate, because the extraction of the T_0 thermal contribution from the static EOS is not exact. Secondly, in the extreme high temperature region, the results of $\alpha(T)$ and $C_P(T)$ from our model match the measured results even better than the Wu *et al.*'s[20] model with classical treatment of the anharmonicity, which shows the validity of our anharmonic model. Thirdly, in the low temperature region, we compared with the experimental data the results of $C_V(T)$ from ours, Wu *et al.*'s,[23] and Tange *et al.*'s[25] models. It is revealed that our model fits the measured results excellently, which proves the accuracy of our analytic pseudo-Debye model.

References

[1] Rose J H, Smith J R and Ferrante J 1983 *Phys. Rev.* B **28** 1835

[2] Rose J H, Smith J R, Guinea F and Ferrante J 1984 *Phys. Rev.* B **29** 2963

[3] Vinet P, Smith J R, Ferrante J and Rose J H 1987 *Phys. Rev.* B **35** 1945

[4] Baonza V G, Cáceres M and Núñez J 1995 *Phys. Rev.* B **51** 28

[5] Baonza V G, Taravillo M, Cáceres M and Núñez J 1996 *Phys. Rev.* B **53** 5252

[6] Holzapfel W B 2003 *Phys. Rev.* B **67** 026102

[7] Li J H, Liang S H, Guo H B and Liu B X 2005 *Appl. Phys. Lett.* **87** 194111

[8] Li J H, Liang S H, Guo H B and Liu B X 2007 *J. Alloy. Compd.* **431** 23

[9] Qin T, Drautz T and Pettifor D G 2008 *Phys. Rev.* B **77** 220103(R)

[10] Qin T, Drautz T and Pettifor D G 2008 *Phys. Rev.* B **78** 214108

[11] Sun J, Wu Q, Cai L and Jing F 2006 *Physica* B **371** 257

[12] Hu J, Sun J X, Chen X M and Cai L C 2010 *Acta Phys. Sin.* **59** 3384 (in Chinese)

[13] Tian R G and Sun J X 2011 *Chin. Phys.* B **20** 080508

[14] Zhang D, Sun J and Zhao Y 2011 *Physica* B **406** 1276

[15] Jin K, Li X, Wu Q, Geng H, Cai L, Zhou X and Jing F 2010 *J. Appl. Phys.* **107** 113518

[16] Anderson O L and Zou K 1990 *J. Phys. Chem. Ref. Data* **19** 69

[17] Matsui M, Parker S C and Leslie M 2000 *Am. Mineral.* **85** 312

[18] Karki B B, Wentzcovitch R M, de Gironcoli S and Baroni S 2000 *Phys. Rev.* B **61** 8793

[19] Oganov A R and Dorogokupets P I 2003 *Phys. Rev.* B **67** 224110

[20] Liu Z J, Cheng X L, Zhang H and Cai L C 2004 *Chin. Phys.* B **13** 384

[21] Wang Y, Liu Z K, Chen L Q, Burakovsky L and Ahuja R 2006 *J. Appl. Phys.* **100** 023533

[22] Dorogokupets P I and Oganov A R 2007 *Phys. Rev.* B **75** 024115

[23] Wu Z Q, Wentzcovitch R M, Umemoto K, Li B S, Hirose K and Zheng J C 2008 *J. Geophys. Res.* **113** B06204

[24] Sun X W, Liu Z J, Chen Q F, Song T and Wang C W 2009 *Chin. Phys.* B **18** 5001

[25] Tange Y, Nishihara Y and Tsuchiya T 2009 *J. Geophys. Res.* **114** B03208

[26] Dorogokupets P I 2010 *Phys. Chem. Mineral.* **37** 677

[27] Duffy T S, Hemley R J and Mao H K 1995 *Phys. Rev. Lett.* **74** 1371

[28] Zha C S, Mao H K and Hemley R J 2000 *Proc. Natl. Acad. Sci. USA* **97** 13494

[29] Fei Y W 1999 *Am. Mineral.* **84** 272

[30] Dewaele A and Fiquet G 2000 *J. Geophys. Res.* **105** 2869

[31] Speziale S, Zha C S and Duffy T S 2001 *J. Geophys. Res.* **106** 515

[32] Zhang L and Gong Z 2006 *Chin. Phys. Lett.* **23** 3049

[33] Jacobsen S D, Holl C M, Adams K A, Fischer R A, Martin E S, Bina C R, Lin J F, Prakapenka V B, Kubo A and Dera P 2008 *Am. Mineral.* **93** 1823

[34] Hirose K, Sata N, Komabayashi T and Ohishi Y 2008 *Phys. Earth Planet. Inter.* **167** 149

[35] Gillet P, Matas J, Guyot F and Ricard Y 1999 *Microscopic Properties and Processes in Minerals, NATO Science Series* C Vol. 543 (Dordrecht: Kluwer) p. 71

[36] Oganov A R and Dorogokupets P I 2004 *J. Phys.*: *Condens. Matter* **16** 1351

[37] Holzapfel W B 2002 *J. Phys.: Condens. Matter* **14** 10525

[38] Shukla R C and Cowley E R 1985 *Phys. Rev.* B **31** 372

[39] Lacks D J and Shukla R C 1996 *Phys. Rev.* B **54** 3266

[40] Al'tshuler L V, Brusnikin S E and Kuzmenkov E A 1987 *Zh. Prikl. Mekh. Tekh. Phys.* **161** 134

[41] Vorobev V S 1996 *High Temp.* **34** 391

[42] Grover R 1971 *J. Chem. Phys.* **55** 3435

[43] Xu X and Zhang W 1986 *Practical Introduction to Equation of State* (Beijing: Science Press) p. 340 (in Chinese)

[44] Beg M M 1976 *Acta Cryst.* **A32** 154

[45] Cohen A J and Gordon R J 1976 *Phys. Rev.* B **14** 4595

[46] Zerr A and Boehler R 1994 *Nature* **371** 506

[47] Fei Y, Li J, Hirose K, Minarik W, Van Orman J, Sanloup C, van Westrenen W, Komabayashi T and Funakoshi K 2004 *Phys. Earth Planet. Inter.* **143–144** 515

[48] Vassiliou M S and Ahrens T J 1981 *Geophys. Res. Lett.* **8** 729

[49] Duffy T S and Ahrens T J 1993 *Geophys. Res. Lett.* **20** 1130

[50] Marsh S P 1980 *LASL Shock Hugoniot Data* (Berkeley: University of Califonia Press)

[51] Ponkratz U and HolzapfeL W B 2004 *J. Phys.: Condens. Matter* **16** S963

[52] Anderson O L 1995 *Equations of State of Solids for Geophysics and Ceramic Science* (Oxford: Oxford University Press)

[53] Touloukian Y S, Kirby R K, Taylor R E and Desai P D 1975 *Thermophysical Properties of Matter* Vol. 12 (New York: Plenum)

[54] Simmons G and Wang H 1970 *Single Crystal Elastic Constants and Calculated Aggregate Properties: A Handbook* (Cambridge MA: MIT Press)

[55] Touloukian Y S, Kirby R K, Taylor R E and Lee T Y R 1977 *Thermophysical Properties of Matter* Vol. 13 (New York: Plenum)

[56] Fiquet G, Richet P and Montagnac G 1999 *Phys. Chem. Miner.* **27** 103

[57] Chase M W Jr 1998 *NIST–JANAF Thermochemical Tables, J. Phys. Chem. Ref. Data*, Monograph, No. 9, Am. Chem. Soc., Am. Inst. Phys., Nat. Inst. Stand. Tech.